

# Solid Optical Fiber With Tunable Bandgaps Based on Curable Polymer Infiltrated Photonic Crystal Fiber

Bing Sun, Wei Wei, Chao Wang, Changrui Liao, Jing Xu, Hongdan Wan, Lin Zhang, Zuxing Zhang, and Yiping Wang, *Senior Member, IEEE*

**Abstract**—We demonstrated the realization and characterization of a solid photonic bandgap fiber (SPBF) with a compact size of about 10 mm and a high wavelength sensitivity of up to  $-4.034 \text{ nm}/^\circ\text{C}$  by means of fully infiltrating an ultraviolet curable polymer with a high refractive index of 1.515 into air holes of a photonic crystal fiber (PCF). To the best of our knowledge, it was the first time that the SPBF with tunable bandgaps was fabricated in the conventional index-guiding PCF. Compared with conventional fluid filled PBFs, the proposed SPBF can be stable to temperature and other environmental effects and maintain a large extinction ratio of more than 30 dB within a broad wavelength. The splicing between the SPBF and single mode fibers has been solved. Moreover, it is observed that the bandwidth of bandgap (G2) gradually broadens with the increase in temperature.

**Index Terms**—Microstructured optical fibers, photonic bandgaps fiber, tunable bandgaps, sensor.

## I. INTRODUCTION

PHOTONIC crystal fiber (PCF) [1], a type of microstructured optical fiber (MOF) where a regular-hexagonal lattice of hollow channels is arrayed symmetrically around a central silica core, has resulted in a number of novel devices and sensing applications. In recent years, as a relatively new member of the family of MOFs, all-solid photonic bandgap fibers have attracted great attention because of their easiness to fabricate, splicing with single mode fibers, all-solid structure and promising potential application [2]–[6]. Note that the locations of these formed bandgaps are spectrally determined by the resonance properties of the high-index inclusions. And the high-index rods including into silica background are usually Ge-doped ones. We have to admit that the Ge-doped rods have a graded index profile with a maximum  $\Delta n$  of 2.03%, which forms a low index contrast,

Manuscript received May 9, 2016; revised June 13, 2016; accepted June 28, 2016. Date of publication June 29, 2016; date of current version November 22, 2016. This work was supported in part by the National Natural Science Foundation of China under Grant 61505119, Grant 61405125, and Grant 11174064, in part by the Brain Gain Foundation of Nanjing University of Posts and Telecommunications under Grant NY215040, and in part by the Distinguished Professor Project of Jiangsu under Grant RK002STP14001. (*Corresponding author: Zuxing Zhang.*)

B. Sun, W. Wei, H. Wan, and Z. Zhang are with the School of Optoelectronic Engineering, Nanjing University of Posts and Telecommunications, Nanjing 210023, China (e-mail: b.sun@njupt.edu.cn; weiwei@njupt.edu.cn; hdwan@njupt.edu.cn; zxzhang@njupt.edu.cn).

C. Wang, C. Liao, and Y. Wang are with the Key Laboratory of Optoelectronic Devices and Systems of Ministry of Education and Guangdong Province, College of Optoelectronic Engineering, Shenzhen University, Shenzhen 518060, China (e-mail: 3752601@qq.com; cliao@szu.edu.cn; ypwang@szu.edu.cn).

J. Xu is with the Optical Communications Laboratory, Ocean College, Zhejiang University, Zhejiang 316021, China (e-mail: jxu-optics@zju.edu.cn).

L. Zhang is with the Aston Institute of Photonic Technologies, Aston University, Birmingham B4 7ET, U.K. (e-mail: l.zhang@aston.ac.uk).

Color versions of one or more of the figures in this paper are available online at <http://ieeexplore.ieee.org>.

Digital Object Identifier 10.1109/JLT.2016.2586584

and then results in a low-extinction-ratio bandgap. Although the all-solid photonic bandgap fiber with a high index contrast (e.g.  $\Delta n = 0.23$ ) has been fabricated by the well-known stack-and-draw technique [2], [3], [7], it is limited by the required pairs of glasses with closely similar softening temperatures and thermal expansion coefficients.

Fortunately, bandgaps with a high extinction ratio can be realized with infiltration of fluids into air holes of PCFs [8], [9]. And the infiltration of various materials into the cladding, such as refractive index matched liquids [9], liquid crystals [8], [10]–[12], metals [13], ferrofluids [14]–[16], polymers [17], [18], and glasses [19], [20], makes it possible to create highly tunable fiber devices. However, those fibers assisted with fluid filling are being unstable to temperature and other environmental effects. In special, the liquid surface of the liquid infiltrated PCF device at the liquid-air interface fluctuates randomly, results in a poor temporal stability.

In this paper we report the realization and characterization of a solid optical fiber by the use of a polymer material infiltrating into PCF. Note that the periodic alternating layers of dielectric material give rise to two-dimensional Bragg scattering forming a photonic band gap in the cladding. And frequencies which lie within the photonic bandgap are not allowed to propagate within the cladding. The bandgaps of the cladding spontaneously depend on the refractive index of the inclusions in the PCF, i.e. the thermally tunable polymer. In fact, the SPBF can be easily fabricated owing to the polymer utilized is an ultraviolet (UV) curable liquid. Firstly, the splicing problem of the SPBF is solved according to the optimized splicing parameters. Secondly, we have numerically simulated and experimentally observed the guiding mechanism transformation between modified total internal reflection and photonic bandgap guidance. Finally, we investigate the response of the SPBF to temperature ranging from 25 °C to 95 °C.

## II. NUMERICAL SIMULATION OF BANDGAP LOCATION AND EXPERIMENTAL RESULTS

As shown in Fig. 1, a large-mode-area PCF (LAM-10, <http://www.nktpotonics.com>) is employed. The PCF is composed of hexagonally arrayed cladding holes with a diameter of 3.3  $\mu\text{m}$  while the core is formed by omitting an air hole in the center. And the pitch of the PCF is 7.4  $\mu\text{m}$ .

Here, we take advantage of a commercially available Norland Optical Adhesive, i.e., NOA65. The NOA65 is a clear, colorless, liquid photopolymer, whose viscosity is about 300 cps at room temperature. Frankly speaking, infiltrating NOA65 into air holes of PCFs is a complicated and time-consuming process, owing to not only its viscosity but the time required for capillary filling grows as the square of the length [21]. To solve it, we submerge one end-facet of the PCF into a liquid bottle full of NOA65, while leaving the other end-facet connected to an injection

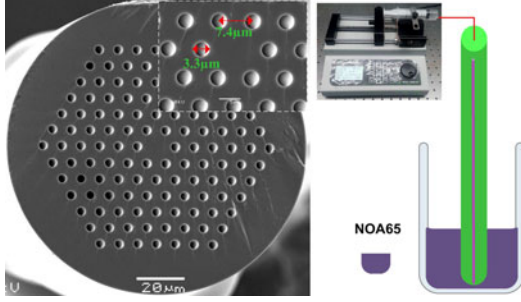


Fig. 1. (Left) Cross-sectional SEM images of the PCF employed. (Right) Schematic of PCF fluid filling set-up assisted with Longer Pump.

TABLE I  
SPlicing PARAMETERS FOR A COMMERCIAL FUSION SPLICER (FUJIKURA-60S)

Parameters	Values	Units
Prefusion power	standard-25	bit
Prefusion time	180	ms
Overlap	6	$\mu\text{m}$
Fusion power	standard-30	bit
Fusion time	300	ms
Offset	-30	$\mu\text{m}$

syringe to apply pressure to the fluid. As a result, the filling time can be significantly reduced owing to the existence of the pressure difference between the PCF end-facets. We utilize a commercial machine (LSP02-2A, <http://www.longerpump.com.cn>), where an electrically controlled moving stage has been exploited. Considering that bubbles may undesirably form and result in a discontinuous strand of fluid, the flow rate cannot be too rapid. As a result, it takes one hour for filling material to fill a  $\sim 50$ -mm long PCF in this experiment.

Next, we focus on solving the splicing difficulty between single mode fibers (SMFs) and the fully NOA65-filled PCF. We know that the high temperature involved during fusion splicing will induce the polymer, i.e., NOA65 to boil and evaporate. As a result, it eventually leads to a bad physical strength. In the previous report [8], we take advantage of the optimized splicing parameters of a commercial fusion splicer (Fujikura-60S) to implement the splicing between liquid crystal filled PCFs and SMFs. To solve it, optimized splicing parameters for the Fujikura-60S are listed in Table I. For our fiber device, the insertion losses mainly derived from splicing joints losses at the input/output and absorption loss of the polymer in the holes. In fact, the couplings between the filled and unfilled sections of the PCF can also lead to loss. Furthermore, the mode field mismatch resulting from an index guiding mode and PBG guiding mode at the splices would further bring losses.

Fortunately, the NOA65-filled PCF can be cured by UV light (a wavelength from 320 nm to 380 nm) with an intensity of approximately  $270 \text{ mW/cm}^2$  in this experiment, as shown in Fig. 2. In this UV-curing process, the NOA65 with a refractive index of about 1.515 is gradually transformed into a solid polymer with a refractive index of 1.524 [22]. Consequently, a solid photonic bandgap fiber (SPBF) with a compact size of about 10 mm has been fabricated. Such a compact size can probably be attributed to the higher refractive index ( $n = 1.524$ ) of the polymer employed.



Fig. 2. Schematic of the NOA65-filled PCF. The insets side image shows the fusion joint of the NOA65-filled PCF with a single mode fiber.

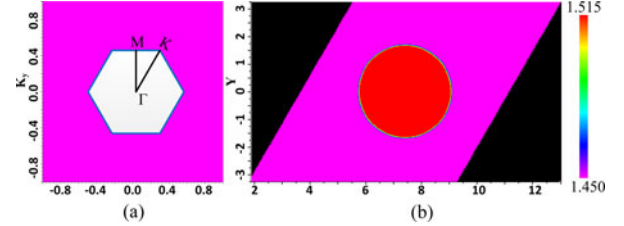


Fig. 3. (a) First Brillouin zone and k-path for a hexagonal lattice. (b) Index profile for the single unit cell.

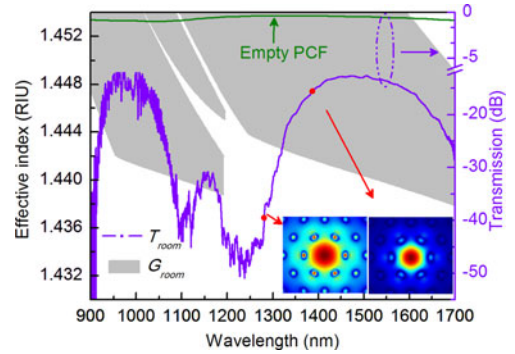


Fig. 4. Calculated bandgap maps (gray color) for the SPBF and the transmission spectra of the filled (purple line) and unfilled PCF (green line). Inset: Calculated mode field distributions of the SPBF at 1290 and 1400 nm wavelength.

A full-vectorial plane wave method (FV-PWM) is applied to calculate the location of photonic bandgaps of the cladding unit cell, i.e., effective-index curves, for the fundamental mode guided in the SPBF at a temperature of  $25^\circ\text{C}$ . We first solve the frequency eigenvalues of the vector Helmholtz equation, and then calculate the band structure of the SPBF by considering the irreducible first Brillouin zone of the hexagonal fiber lattice, where the number of plane waves used to resolve the unit cell is  $256 \times 256$  and  $\beta\Lambda$  is scanned in steps of 0.05. The first Brillouin zone of triangular lattice in cladding of SPBF is shown in Fig. 3(a), where the axis is considered to be parallel to the  $\Gamma$ -M direction owing to that the  $x$ - $y$  plane is periodic. Furthermore, a single primitive unit cell, as shown in Fig. 3(b), is chosen.

As shown in Fig. 4, it is evident that three bandgaps (denoted in gray color) are observed in the calculated modal maps at the temperature of  $25^\circ\text{C}$  within the wavelength range from 900 to 1700 nm, where the thermo-optic effect of the pure silica background is taken into consideration in the calculations. Furthermore, the transmission spectrum of the SPBF can be measured by connecting a white-light source (NKT SuperK Compact) and an optical spectrum analyzer (YOKOGAWA AQ6370C). We also found that three bandgaps occurred within the whole wavelength range in accordance with the simulation. Some slight

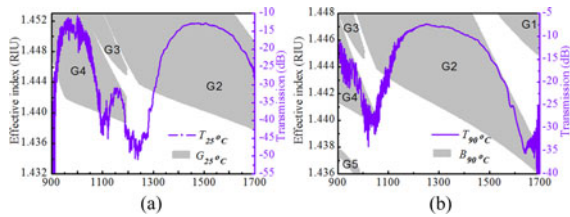


Fig. 5. Measured transmission spectra and the corresponding bandgap maps of the SPBF at a temperature of (a) 25 °C and (b) 90 °C.

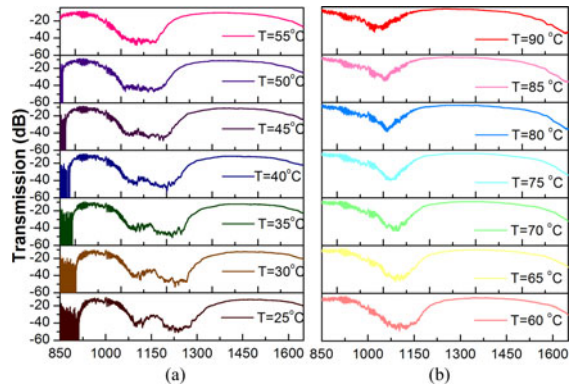


Fig. 6. The transmission spectra of the SPBF corresponding to variations in temperature ranging from 25 °C to 90 °C.

discrepancy in the bandgaps location is attributed to the fact that the material property of the polymer, i.e., NOA65 is not thoroughly researched. Intuitively, the operation of the SPBF may be explained in terms of antiresonant reflecting optical waveguides (ARROW), where individual rods (NOA65-filled holes) form isolated waveguides. Furthermore, the ARROW model predicts the spectral stopbands to be positioned at wavelengths corresponding to modal cutoff wavelengths of a single NOA65-filled hole. The insets shown in Fig. 4 illustrate that light at wavelengths near the cutoff wavelengths, i.e.,  $\lambda = 1290$  nm of the individual rods' modes can couple to these rods while the cladding becomes transparent to the light and light cannot remain confined in the core. Between cutoff wavelengths, i.e.,  $\lambda = 1400$  nm, however, light cannot couple to the resonances of the high-index inclusions and thus remains in the core.

We then investigate the temperature response of the SPBF by placing it in a column oven, where the temperature is raised from 25 °C to 90 °C in step of 10 °C. As shown in Fig. 5, three bandgaps, i.e., G2, G3 and G4, appears at the temperature of 25 °C, while another bandgaps, i.e., G1 and G5, located at the shortest and longest wavelength are gradually observed at the temperature of 90 °C. As the temperature is increased, the edge wavelengths of the bandgap shift toward a shorter wavelength, i.e., “blue” shift, due to a negative thermo-optic coefficient ( $-1.83 \times 10^{-4}/^{\circ}\text{C}$ ) of the polymer, i.e., NOA65 [23]. As shown in Fig. 6, we tend to attribute the decline in wavelength of the G2 edges at higher temperatures to the negative thermo-optic coefficient of the NOA65 owing to that the cutoff wavelengths of the high-index inclusion's modes shift toward a shorter wavelength with the increased temperature. Moreover, the simulation results show, in general, good qualitative agreement with the experimental measurements.

In order to evaluate quantitatively the temperature-induced shift of this device, we illustrate the wavelength, corresponding to  $-20$  dB, of the left and right edges of the bandgap. This is

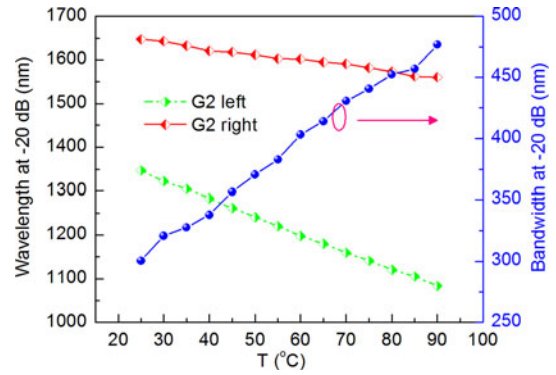


Fig. 7. Wavelengths, corresponding to a transmission of  $-20$  dB, at the left and right edges of the G2, and the bandwidth of G2 versus the temperature.

because it is very difficult to measure the center wavelength of each bandgap. In this experiment, we characterize the bandgap 2 (G2) at different temperature for convenience's sake. It can be seen from Fig. 7 that the left edges of G2 linearly shifted toward a shorter wavelength, i.e., “blue” shift with a high sensitivity of  $-4.034$  nm/ $^{\circ}\text{C}$  while the right edges of G2 also present a “blue” shift with a lower sensitivity of  $-1.319$  nm/ $^{\circ}\text{C}$  during the temperature rise. The temperature sensitivity of the reported AS-PCF is close to 2 times higher than that of the liquid-filled PCF [24]. Note that the proposed AS-PCF takes advantage over the previous results [25], [26] in regard to the temperature sensitivity. As a result, the bandwidth of G2 gradual broadens with the temperature rise owing to the different sensitivity between the left and right edges of G2.

### III. CONCLUSION

In this paper, we presented a SPBF fabricated from the conventional index-guiding PCF with a curable polymer-filled cladding. The polymer inclusions introduce a high index contrast between the core and the cladding and consequently lead to lots of bandgaps. We simulated and measured the transmission spectrum from 900 to 1700 nm and recorded the response of the SPBF to temperature. The results illustrated our proposed SPBF is wavelength-tunable with a sensitivity of up to  $-4.034$  nm/ $^{\circ}\text{C}$  and has a large extinction ratio of more than 30 dB (G2). In conclusion, the proposed SPBF provides a new and simple highway for guidance of light and appears to extremely temporal stability.

### REFERENCES

- [1] P. S. J. Russell, “Photonic-crystal fibers,” *J. Lightw. Technol.*, vol. 24, no. 12, pp. 4729–4749, Dec. 2006.
- [2] F. Luan *et al.*, “All-solid photonic band gap fiber,” *Opt. Lett.*, vol. 29, no. 20, pp. 2369–2371, 2004.
- [3] A. Argyros, T. Birks, S. Leon-Saval, C. M. Cordeiro, F. Luan, and P. S. J. Russell, “Photonic bandgap with an index step of one percent,” *Opt. Express*, vol. 13, no. 1, pp. 309–314, 2005.
- [4] G. Bouwmans, L. Bigot, Y. Quiquempois, F. Lopez, L. Provino, and M. Douay, “Fabrication and characterization of an all-solid 2D photonic bandgap fiber with a low-loss region ( $<20$  dB/km) around 1550 nm,” *Opt. Express*, vol. 13, no. 21, pp. 8452–8459, 2005.
- [5] J. M. Stone *et al.*, “An improved photonic bandgap fiber based on an array of rings,” *Opt. Express*, vol. 14, no. 213, pp. 6291–6296, 2006.
- [6] M. A. Schmidt, N. Granzow, N. Da, M. Peng, L. Wondraczek, and P. St. J. Russell, “All-solid bandgap guiding in tellurite-filled silica photonic crystal fibers,” *Opt. Lett.*, vol. 34, no. 13, pp. 1946–1948, 2009.
- [7] T. A. Birks, F. Luan, G. J. Pearce, A. Wang, J. C. Knight, and D. M. Bird, “Bend loss in all-solid bandgap fibres,” *Opt. Express*, vol. 14, no. 12, pp. 5688–5698, 2006.

- [8] Y. Liu *et al.*, "Compact tunable multibandpass filters based on liquid-filled photonic crystal fibers," *Opt. Lett.*, vol. 39, no. 7, pp. 2148–2151, 2014.
- [9] B. Sun *et al.*, "Broadband thermo-optic switching effect based on liquid crystal infiltrated photonic crystal fibers," *IEEE Photon. J.*, vol. 7, no. 4, pp. 6802207–1, Aug. 1, 2015.
- [10] A. Lorenz and H.-S. Kitzerow, "Efficient electro-optic switching in a photonic liquid crystal fiber," *Appl. Phys. Lett.*, vol. 98, no. 24, p. 241106, Nov. 13, 2011.
- [11] J. Du, Y. Liu, Z. Wang, B. Zou, B. Liu, and X. Dong, "Liquid crystal photonic bandgap fiber: different bandgap transmissions at different temperature ranges," *Appl. Opt.*, vol. 47, no. 29, pp. 5321–5324, Oct. 10, 2008.
- [12] M. Wahle and H.-S. Kitzerow, "Measurement of group velocity dispersion in a solid-core photonic crystal fiber filled with a nematic liquid crystal," *Opt. Lett.*, vol. 39, no. 16, pp. 4816–4819, Aug. 11, 2014.
- [13] H. W. Lee, M. A. Schmidt, and P. St. J. Russell, "Excitation of a nanowire 'molecule' in gold-filled photonic crystal fiber," *Opt. Lett.*, vol. 37, no. 14, pp. 2946–2948, 2012.
- [14] A. Candiani, M. Konstantaki, W. Margulis, and S. Pissadakis, "A spectrally tunable microstructured optical fiber Bragg grating utilizing an infiltrated ferrofluid," *Opt. Express*, vol. 18, no. 24, pp. 24654–24660, 2010.
- [15] A. Mahmood, V. Kavungal, S. S. Ahmed, G. Farrell, and Y. Semenova, "Magnetic-field sensor based on whispering-gallery modes in a photonic crystal fiber infiltrated with magnetic fluid," *Opt. Lett.*, vol. 40, no. 21, pp. 4983–4986, 2015.
- [16] H. V. Thakur, S. M. Nalawade, S. Gupta, R. Kitture, and S. N. Kale, "Photonic crystal fiber injected with Fe<sub>3</sub>O<sub>4</sub> nanofluid for magnetic field detection," *Appl. Phys. Lett.*, vol. 99, no. 16, 2011.
- [17] P. S. Westbrook, B. J. Eggleton, R. S. Windeler, A. Hale, T. A. Strasser, and G. L. Burdge, "Cladding-mode resonances in hybrid polymer-silica microstructured optical fiber gratings," *IEEE Photon. Technol. Lett.*, vol. 12, no. 5, pp. 495–497, May 2000.
- [18] C. Markos, K. Vlachos, and G. Kakarantzas, "Broadband guidance in a hollow-core photonic crystal fiber with polymer-filled cladding," *IEEE Photon. Technol. Lett.*, vol. 25, no. 20, pp. 2003–2006, Oct. 2013.
- [19] N. Granzow, P. Uebel, M. A. Schmidt, A. S. Tverjanovich, L. Wondraczek, and P. S. J. Russell, "Bandgap guidance in hybrid chalcogenide-silica photonic crystal fibers," *Opt. Lett.*, vol. 36, no. 13, pp. 2432–2434, 2011.
- [20] I. Konidakis, G. Zito, and S. Pissadakis, "Photosensitive, all-glass AgPO<sub>3</sub>/silica photonic bandgap fiber," *Opt. Lett.*, vol. 37, no. 13, pp. 2499–2501, 2012.
- [21] K. Nielsen, D. Noordegraaf, T. Sorensen, A. Bjarklev, and T. Hansen, "Selective filling of photonic crystal fibres," *J. Opt. A, Pure Appl. Opt.*, vol. 7, no. 8, pp. L13–L20, Aug. 2005.
- [22] C.-L. Lee, L.-H. Lee, H.-E. Hwang, and J.-M. Hsu, "Highly sensitive air-gap fiber Fabry–Perot interferometers based on polymer-filled hollow core fibers," *IEEE Photon. Technol. Lett.*, vol. 24, no. 2, pp. 149–151, Jan. 2012.
- [23] K. R. Sohn and G.-D. Peng, "Mechanically formed loss-tunable long-period fiber gratings realized on the periodic arrayed metal wires," *Opt. Commun.*, vol. 278, no. 1, pp. 77–80, 2007.
- [24] Y. Liu *et al.*, "Compact tunable multibandpass filters based on liquid-filled photonic crystal fibers," *Opt. Lett.*, vol. 39, no. 7, pp. 2148–2151, 2014.
- [25] Y. Geng, X. Li, X. Tan, Y. Deng, and X. Hong, "Compact and ultrasensitive temperature sensor with a fully liquid filled photonic crystal fiber Mach–Zehnder interferometer," *IEEE Sens. J.*, vol. 14, no. 1, pp. 167–170, Jan. 2014.
- [26] G. Yin *et al.*, "Simultaneous refractive index and temperature measurement with LPPG and liquid-filled PCF," *IEEE Photon. Technol. Lett.*, vol. 27, no. 4, pp. 375–378, Feb. 2015.

**Bing Sun** was born in Jiujiang, China, in 1986. He received the B.S. degree in optical information science and technology from Changchun University of Science and Technology, Changchun, China, and the Ph.D. degree in mechanical engineering from Jiangsu University, Zhenjiang, China, in 2008 and 2013, respectively. His Ph.D. thesis is focused on the design of photonic crystal fiber devices. In July 2013, his dissertation was awarded the prestigious "Excellent Doctoral Dissertation" Prize at Jiangsu University in 2013. From 2013 to 2015, as a Postdoctoral Research Fellow at Shenzhen University, he experimentally developed fluid filled photonic crystal fiber for application in optical fiber sensors. Since 2015, he has been a Lecturer at Nanjing University of Posts and Telecommunications, Nanjing, China. His research interests include optical fiber sensors, fiber Bragg gratings, and fluid filled photonic crystal fiber. He has authored or coauthored ten patent applications, and more than 40 journal and conference papers.

**Wei Wei** received the B.S., M.S., and Ph.D. degrees from Xi'an Jiaotong University, Xi'an, China, in 1982, 1987, and 1998, respectively. She is currently the Dean of the School Optoelectronic Engineering, Nanjing University of Posts and Telecommunications, Nanjing, China. During 1999–2001, she was invited as a Visiting Professor at Waseda University and was offered a JISA fellowship from the Institute of Scientific and Industrial Research, Osaka University, Ministry of International Trade and Industry, Japan. From 2002 to 2004, she was the Director of the Department of Information Science, National Natural Science Foundation of China, In-Charge of floating projects.

**Chao Wang** received the Bachelor's and Master's degrees from the School of Optical and Electronic Information, Huazhong University of Science and Technology, Wuhan, China, in 2002 and 2005 respectively, and the Ph.D. degree in fiber optics from the Department of Electrical Engineering, Hong Kong Polytechnic University, Hung Hom, Hong Kong, in 2013. In 2016, he joined as an Associate Professor at the School of Electrical Engineering, Wuhan University. His research interests include optical fiber sensors and devices, gas and liquid detection, and condition monitoring in electrical power system.

**Changrui Liao** received the Ph.D. degree in electrical engineering from the Hong Kong Polytechnic University, Hung Hom, Hong Kong, in 2012. He is currently an Assistant Professor with Shenzhen University, Shenzhen, China. His current research interests include optical fiber sensors and femtosecond laser micromachining. He has authored or coauthored ten patent applications and more than 60 journal and conference papers.

**Jing Xu** received the M.S. degree in information engineering from Jinan University, Guangzhou, China, and the Ph.D. degree in information engineering from The Chinese University of Hong Kong, Hong Kong, in 2011. His current research interests include optical sensors and sensor networks and underwater optical wireless communications.

**Hongdan Wan**, biography not available at the time of publication.

**Lin Zhang** received the undergraduate and Master's degrees from Suzhou University, Suzhou, China, in 1978 and 1986, respectively, and the Ph.D. degree from Sussex University, Sussex, U.K., in 1990.

From 1990 to 1994, she was a Research Fellow at the Department of Physics, Sussex University, working in the field of passive and active planar waveguide devices. In 1994, she joined as a Lecturer at the Photonics Research Group, Department of Electronic Engineering, Aston University, Birmingham, U.K. Her current research interests include the field of fiber grating technology and its applications in telecommunications and optical sensing. She has been extensively involved in four U.K. DTI and EPSRC LINK programs and many other EPSRC-, EU-, and DERA-funded research projects. She has authored and coauthored more than 400 papers in peer-review journals and international conferences.

**Zuxing Zhang** received the Ph.D. degree from Shanghai Jiao Tong University, Shanghai, China. He is currently a Professor at the College of Opto-electronic Engineering, Nanjing University of Posts and Telecommunications, Nanjing, China. His research interests include fiber lasers, fiber sensors nonlinear optics, and optical communications.

**Yiping Wang** (SM'11) received the B.Eng. degree in precision instrument engineering from the Xi'an Institute of Technology, Xi'an, China, in 1995, and the M.S. degree in precision instrument and mechanism and the Ph.D. degree in optical engineering from Chongqing University, Chongqing, China, in 2000 and 2003, respectively.

He is currently a Distinguished Professor and a Pearl River Scholar at the College of Optoelectronic Engineering, Shenzhen University, Shenzhen, China. He has authored or coauthored one book, nine patent applications, and more than 150 journal and conference papers with a SCI citation of more than 1200 times. He is a Senior Member of the Optical Society of America and the Chinese Optical Society. He received the prestigious award of the National Excellent Doctoral Dissertation of China.